Numerical Investigations of the Impact of Temperature Fluctuations on Lean Premixed Flames

C. Schrödinger*, C. O. Paschereit* and M. Oevermann**

* Institut für Strömungsmechanik und Technische Akustik, TU Berlin, Germany
** Division of Combustion, Chalmers University of Technology, Gothenburg, Sweden

1 Introduction

Lean premixed combustion is used in gas turbine processes being able to operate under moderate temperatures in order to reduce emissions, such as NO_x and CO. A major drawback of lean premixed flames, especially when turbulent, is their susceptibility to combustion instabilities. These instabilities may be driven by various effects and their interaction, e.g. coherent flow structures [1], flame surface variations [2] and enthalpy disturbances (equivalence ratio or temperature fluctuations) [3].

The influence of enthalpy fluctuations on premixed flames and the coupling with acoustic waves has been studied theoretically and experimentally [3, 4]. These studies concentrate on perturbations in fuel mass fraction although the developed theories hold for both, equivalence ratio and temperature fluctuations. Investigations on temperature perturbations in the unburned mixture are rare.

Temperature fluctuations might be introduced by turbulent transport [5], azimuthal interactions as they may occur in annular combustion chambers, or entropy waves in configurations with flue gas recirculation or sequential combustion. The effect of temperature fluctuations on NOx formation regarding the thermal pathway has been studied by Jones [6] whereas Böhm et al. [7] concentrated on the influence of stratification on lean premixed combustion.

In the present paper, the impact of temperature fluctuations on one-dimensional laminar and highly turbulent lean premixed flames is evaluated. Most modeling approaches on enthalpy fluctuations consider the well-stirred reactor or the wrinkled flamelets combustion regime. The current turbulent simulations on the other hand examine flames in the distributed reaction zone regime employing the Linear Eddy Model [8] which allows for temporally and spatially resolved parametric studies.

2 Numerical methods

2.1 The Linear Eddy Model

The Linear Eddy Model (LEM) developed by Kerstein [8] resolves all physically relevant length and time scales on a one-dimensional domain. The main idea behind this approach is to treat molecular diffusion processes and turbulent advection separately. Molecular diffusion is implemented deterministically whereas turbulent stirring is represented by a sequence of statistically independent rearrangement events interpreted as turbulent eddies. They are expressed by triplet maps, which compress the scalar field within a chosen segment by a factor of three. The original field is then replaced with three adjacent copies of the compressed field, with the middle copy spatially

Correspondence to: christina.schroedinger@tu-berlin.de

inverted. The maps are measure-preserving and do not introduce discontinuities into the scalar profiles. Each event is governed by three variables: the time when the eddy occurs, the location and the size of the eddy. The location is chosen randomly. The size of the eddy is chosen from a distribution of domain sizes which is obtained by applying Kolmogorov scaling laws. Identifying that the rearrangement events induce a random walk of one particle on a line, a rate parameter, λ, with dimensions $[l^{-1}t^{-1}]$ and a pdf describing the length distribution, $f_1(l)$, can be determined. The diffusivity of the random walk is thereby interpreted as the turbulent diffusivity D_t. The eddy occurrence time is sampled from a Poisson process with distribution function $f_2(t)$:

$$\lambda = \frac{54}{5} D_t L^{-3} \frac{\left[1 - (\eta/L)^{-5/3}\right]}{\left[(\eta/L)^{4/3} - 1\right]}, \quad f_1(l) = \frac{-5/3}{L^{-5/3} - \eta^{-5/3}} l^{-8/3}, \quad f_2(t) = \frac{1}{\tau} \exp -t/\tau, \tag{1}$$

where η denotes the Kolmogorov scale, L the integral length scale, and τ the mean eddy occurrence time $< t >= \tau = \frac{1}{\lambda S}$ with S being the size of the one-dimensional domain. Considering Eq. (1) three input parameters are needed for the model, namely the integral length scale L, the Kolmogorov scale η, and the turbulent diffusivity D_t.

The LEM reproduces important key features of turbulent mixing [8] and proved itself to be a valid model in studies in various research fields, amongst them LEM simulations on turbulent premixed combustion and pollutant formation by Smith & Menon [9].

2.2 Code implementation

The code is based on an implementation developed by Lignell et al. [10] for diffusion flames and One Dimensional Turbulence (ODT) [11]. The code was refined to be suitable for one-dimensional turbulent premixed flames employing the Linear Eddy Model. In the following, the code implementation will be described shortly.

The diffusive advancement is implemented using a Lagrangian formulation on an unstructured, self-adapting grid. This implies no mass fluxes across the cell boundaries which leads to expansion and contraction of cells. For discretization of spatial derivatives, central differences are used.

The solution of the ordinary differential equations in time is performed separately. The enthalpy equation is solved explicitly using a first-order Euler method while the species equation is solved implicitly. Therefore, the species equation is split between diffusion and source term using the Strang-splitting method. The integration of the chemical source term is performed with CVODE [12] whereas the diffusion term is integrated using the tridiagonal matrix algorithm (TDMA).

The solution procedure including molecular diffusion and turbulent stirring (triplet mapping) for the case of premixed combustion with outflow boundary conditions (Neumann boundary condition) is implemented such that the eddy time, position and size are computed, the eddy/triplet map is applied, diffusion is updated to the eddy time, and eventually the domain is shifted so that the flame remains at the same position.

When shifting the LEM domain, a new cell at the inflow side is created with predefined inflow properties. The outflow side is cut off to conserve the original domain size. The shifting length is calculated from the displacement speed which is determined for each species α from [13]

$$s_D = \frac{1}{\rho_u (Y_{\alpha,b} - Y_{\alpha,u})} M_\alpha \int \omega_\alpha dx. \tag{2}$$

Indices u and b denote the unburnt and burnt states.

2.3 Combustion mechanism

Detailed reaction mechanisms are necessary to investigate dynamic processes in combustion, especially regarding secondary species such as pollutants NO_x and CO.

The reaction mechanism used in this work is a reduced version derived from the GRI-Mech 3.0 [14]. The mechanism was developed within our working group for lean methane-air combustion at atmospheric conditions including NO_x- and CO-formation. All important NO_x-formation pathways for lean combustion were retained from the original mechanism. The reduced mechanism consists of 23 species and 76 reactions.

Figure 1 shows the validation of the reduced mechanism against the GRI-Mech 3.0. Mass fractions of CO and NO, computed from a reactor network are compared for lean conditions. Furthermore, temperature profiles and laminar burning velocities calculated for one-dimensional laminar flames are displayed. The agreement of the reduced with the original mechanism is overall very good.

The software Cantera [15] is employed to calculate thermodynamic properties, chemical kinetics, and transport processes. Transport properties are determined using the mixture-averaged model.

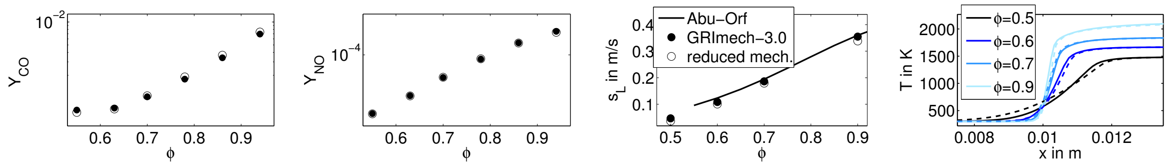

(a) (b) (c) (d)

Figure 1: Validation of the reduced mechanism. (a) CO mass fraction vs. equivalence ratio; (b) NO mass fraction vs. equivalence ratio; (c) burning velocity vs. equivalence ratio in comparison with a correlation by Abu-Orf [16]; (d) temperature profiles for a one-dimensional laminar flame.

3 Results

One-dimensional simulations have been performed for laminar and turbulent cases. A methane-air mixture at an equivalence ratio of 0.6 preheated to 425 K at atmospheric pressure is investigated. The input variables for the Linear Eddy Model, the Kolmogorov and integral lengths as well as the turbulent diffusivity, were set to 1e-4 m, 0.025 m, and 0.01667 m^2/s which corresponds to a turbulence intensity u' of 10 m/s.

3.1 Temperature oscillations

The temperature at the inflow side of the domain is set to sinusoidal oscillations at constant mass fractions and pressure. The simulations are conducted for a frequency range of 20 Hz to 500 Hz and the amplitudes are varied in a wide range for representative frequencies. The computational domain has a length of 0.25 m for turbulent as well as laminar simulations. The flame was initially located at 0.0875 m for the turbulent cases. The amplitudes of temperature fluctuations strongly decrease from inlet to flame front due to heat diffusion. The attenuation thereby depends on the perturbation frequency (Fig. 2(a)). The distance of the laminar flame from the inlet was set in such a way that the amplitude of temperature fluctuations at the flame front corresponds to that of the turbulent case at the same frequency (Fig. 2(b)). The inflow velocity to shift the domain and keep the flame front at the same position was set to the average displacement speeds of the products, H_2O and CO_2. Note that this approach leads to variations in the mass flow and causes an interaction of equivalence ratio oscillations and shifting speed. On the other hand this procedure allows for an approximately constant flame location within the domain. All simulations were run for 1 s to obtain a sufficient number of oscillation periods for averaging. The relative oscillation amplitudes used in the following figures and discussion represent the values at the inlet of the domain.

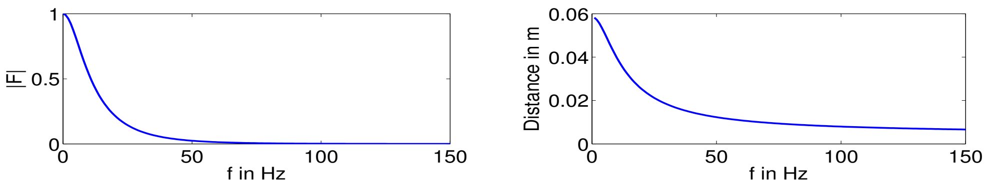

(a) (b)

Figure 2: Diffusive amplitude attenuation for the turbulent case (a) and distance between inlet and flame front for the laminar case corresponding to turbulent distance with the same attenuation (b)

3.2 Influence of temperature oscillations on heat release rate

The heat release rate and especially heat release fluctuations play an important role in gas turbines since they interact with pressure fluctuations and may enhance thermoacoustic instabilities under certain conditions.

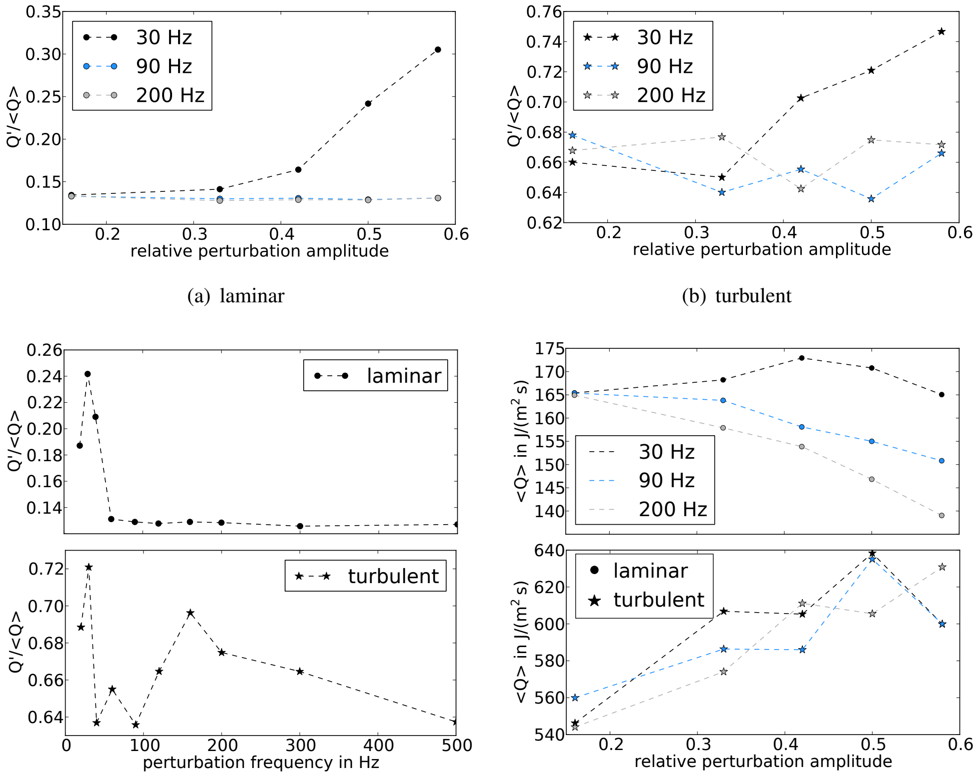

(a) laminar

(b) turbulent

(c)

(d)

Figure 3: Amplitude and frequency dependence of the heat release fluctuations for laminar and turbulent simulations and the influence of forcing amplitude on the mean heat release rate (d).

Figure 3 shows the amplitude and frequency dependence of heat release fluctuations for laminar and turbulent simulations and in addition the influence of forcing amplitude on the mean heat release rate. The heat release fluctuations for laminar and turbulent cases (Fig. 3(a) and 3(b)) show an increase in fluctuation amplitude with forcing amplitude for the 30 Hz case. For the other frequencies no distinct behavior is observable. Figure 3(c) presents the frequency dependence for a relative perturbation amplitude of 0.5 and reveals that the temperature perturbations only have an impact at low frequencies. The frequency range for which an increase in heat release oscillations is observed is thereby wider for the turbulent than for the laminar calculations. The main difference between the laminar and turbulent results is the absolute amplitude of fluctuation which is for the turbulent unforced case more than seven times higher than for the laminar unforced case. The impact of forcing at low frequencies on heat release fluctuations is on the other hand much more distinct for the laminar than for the turbulent cases.

The mean heat release rates plotted against amplitude in Fig. 3(d) exhibit an increase with amplitude for turbulent and a decrease for laminar simulations (except at 30 Hz). In the laminar case thermal diffusion leads to decreasing mean temperature upstream of the flame due to the temperature dependence of the thermal conductivity (thermal diffusion increases with temperature). The temperature decrease increases with amplitude and frequency. The mean density exhibits an opposite trend. The burning velocity on the other hand, which is a convex function of temperature, increases with perturbation amplitude. For the turbulent case turbulent mixing over-weighs thermal diffusion and the inlet mass flow, which corresponds to the inlet velocity (here: $\hat{=}$ burning velocity) times the density, increases. Consequently we see an increase in the mean heat release rate. For the laminar case the thermal diffusion effect dominates and the inlet mass flow as well as the mean heat release rate decrease with amplitude except for the 30 Hz case where the increase in burning velocity over-weighs the diffusive effects in the amplitude range of $0.3 - 0.5$ since the perturbation amplitudes reaching the flame front are higher for low frequencies (Fig. 2(a)).

3.3 Influence of temperature oscillations on emissions of NO and CO

The emissions of NO and CO are subject to strict regulations in modern gas turbine processes. It is therefore important to be able to control emissions and to estimate their behavior under unsteady conditions. The present studies concentrate on the lean combustion regime where modern gas turbines operate due to coexistent low NO and CO emissions. Both pollutants are convex functions of the temperature. The results are evaluated 10 cm downstream of the flame front and represent mean values of the mass fractions.

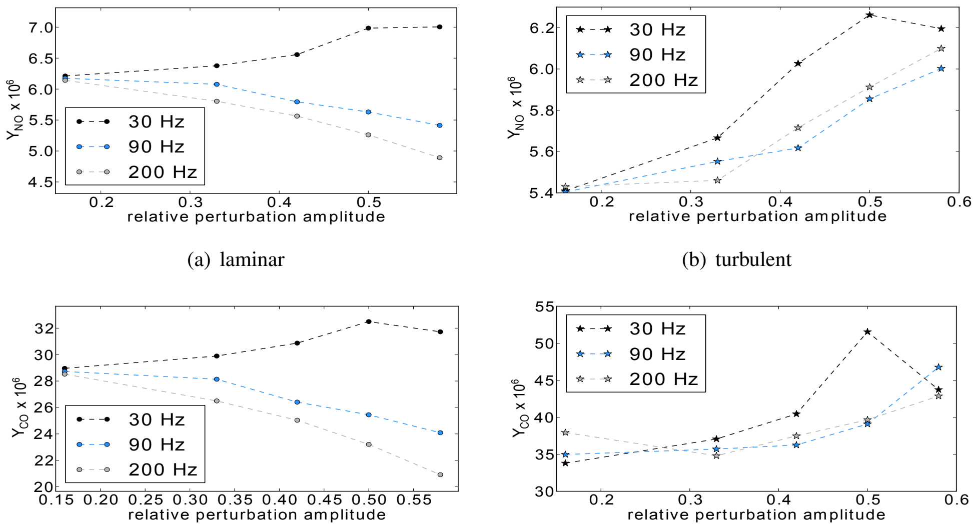

(a) laminar (b) turbulent

(c) laminar (d) turbulent

Figure 4: Influence of forcing amplitude on mean emissions of NO and CO.

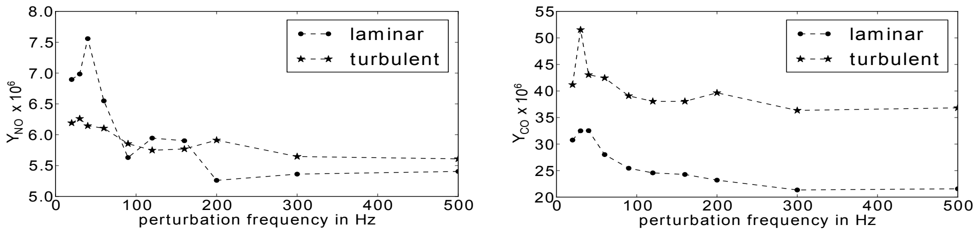

(a) (b)

Figure 5: Influence of forcing frequency on mean emissions of NO and CO at a relative forcing amplitude of 0.5. (a) Mean NO mass fraction; (a) mean CO mass fraction

Figures 4 and 5 show the amplitude respectively frequency dependence of NO and CO. Due to their convex dependence on temperature, NO as well as CO increase with amplitude for the turbulent computations as well as the laminar 30 Hz case. The decrease of emissions for 90 and 200 Hz for the laminar simulations can be attributed to the temperature dependence of the thermal diffusivity and the resulting decrease of mean upstream temperature when thermal diffusion over-weighs the influence of harmonic or turbulent fluctuations (Sec. 3.2). The saturation for high amplitudes which is present in the turbulent and the 30 Hz laminar cases can be explained by the same relation. The impact of temperature oscillations on emissions is strongest for low frequencies but shows a slight increase up to a frequency of 300 Hz.

4 Conclusion

Temperature oscillations might occur in gas turbine combustors and favor or enhance combustion instabilities. On this account it is important to understand the impact of temperature oscillations on flame and emission characteristics. One-dimensional simulations considering laminar as well as turbulent flames have been conducted. The results show that emissions and heat release fluctuations increase with amplitude for a frequency range of 30 to 200 Hz for the turbulent and for low frequencies for the laminar case. Furthermore it was found that two counteracting effects take place when regarding temperature oscillations: a) the mean temperature/density decreases/increases due to the temperature dependence of the thermal conductivity, the stronger the higher the amplitude and frequency; b) the burning velocity (respectively NO and CO), which is a convex function of temperature, increases. Depending on which effect over-weighs, that is harmonic or turbulent fluctuations vs. diffusive effects, the mean heat release, respectively NO/CO emission, increase (turbulent, 30 Hz laminar) or decrease (90, 200 Hz laminar).

Acknowledgment

The authors would like to thank the German Science Foundation (DFG) for financial support.

References

[1] C. O. Paschereit, E. J. Gutmark, and W. Weisenstein, "Coherent structures in swirling flows and their role in acoustic combustion control," *Physics of Fluids*, vol. 11, no. 9, pp. 2667–2678, 1999.

[2] T. Poinsot and S. M. Candel, "A Nonlinear Model for Ducted Flame Combustion Instabilities," *Combustion Science and Technology*, vol. 61, no. 4-6, pp. 121–153, 1988.

[3] T. Lieuwen, Y. Neumeier, and B. T. Zinn, "The Role of Unmixedness and Chemical Kinetics in Driving Combustion Instabilities in Lean Premixed Combustors," *Combustion Science and Technology*, vol. 135, pp. 193–211, 1998.

[4] R. Balachandran, A. Dowling, and E. Mastorakos, "Dynamics of bluff-body stabilised flames subjected to equivalence ratio oscillations," in *Proceeding of the European Combustion Meeting*, 2011.

[5] C. Kortschik, T. Plessing, and N. Peters, "Laser optical investigation of turbulent transport of temperature ahead of the preheat zone in a premixed flame," *Combustion and Flame*, vol. 136, no. 12, pp. 43 – 50, 2004.

[6] W. P. Jones, "The effect of temporal fluctuations in temperature on nitric oxide formation," *Combustion Science and Technology*, vol. 10, no. 1-2, pp. 93–96, 1975.

[7] B. Böhm, J. Frank, and A. Dreizler, "Temperature and mixing field measurements in stratified lean premixed turbulent flames," *Proceedings of the Combustion Institute*, vol. 33, no. 1, pp. 1583 – 1590, 2011.

[8] A. R. Kerstein, "Linear-eddy modelling of turbulent transport. Part 6 Microstructure of diffusive mixing fields," *J. Fluid Mech.*, vol. 231, pp. 361–394, 1991.

[9] T. Smith and S. Menon, "Model simulations of freely propagating turbulent premixed flames," *Symposium (International) on Combustion*, vol. 26, no. 1, pp. 299 – 306, 1996.

[10] D. Lignell, A. Kerstein, G. Sun, and E. Monson, "Mesh adaption for efficient multiscale implementation of one-dimensional turbulence," *Theoretical and Computational Fluid Dynamics*, pp. 1–23, 2012. 10.1007/s00162-012-0267-9.

[11] T. Echekki, A. R. Kerstein, and J. C. Sutherland, *Turbulent Combustion Modeling: Advances, New Trends and Perspectives*, vol. 95 of *Fluid Mechanics and Its Applications*, ch. 11 The One-Dimensional-Turbulence Model, pp. 249–276. Springer, 1st ed., 2011.

[12] S. D. Cohen and A. C.Hindmarsch, "CVODE, a Stiff/Nonstiff ODE Solver in C," *Computers in Physics*, vol. 10, no. 2, pp. 138–143, 1996.

[13] M. Oevermann, H. Schmidt, and A. Kerstein, "Investigation of Autoignition under Thermal Stratification using Linear Eddy Modeling," *Combustion and Flame*, vol. 155, pp. 370–379, 2008.

[14] G. P. Smith, D. M. Golden, M. Frenklach, N. W. Moriarty, B. Eiteneer, M. Goldenberg, C. T. Bowman, R. K. Hanson, S. Song, W. C. G. Jr., V. V. Lissianski, and Z. Qin, "GRI-Mech 3.0, The Gas Research Institute." `http://www.me.berkeley.edu/gri-mech/`.

[15] D. Goodwin, "Cantera: An object-oriented software toolkit for chemical kinetics, thermodynamics, and transport processes." http://code.google.com/p/cantera, 2009.

[16] G. M. Abu-Orf and R. S. Cant, "Reaction rate modelling for premixed turbulent methane-air flames," in *Joint Meeting of the Portuguese, British, Spanish and Swedish Sections of the Combustion Institute, 1-4 April 1996, Madeira, Portugal.*